

# A NEW TRUCK PROTOTYPE FOR TRANSPORTING FLEXIBLE MANIPULATORS

Daniel Feliu-Talegon<sup>(1)</sup>, Juan Carlos Cambera<sup>(1)</sup>, Andres San-Millan<sup>(2)</sup>, Vicente Feliu-Batlle<sup>(3)</sup>

<sup>1</sup> Instituto de Investigaciones Energéticas y Aplicaciones Industriales, University of Castilla-La Mancha.

<sup>2</sup> Institute of Mechanical Engineering, Ecole Polytechnique Fédérale de Lausanne, Lausanne, Switzerland.

<sup>3</sup> Escuela Técnica Superior de Ingenieros Industriales, University of Castilla-La Mancha.

Emails: JuanCarlos.Cambera@alu.uclm.es, Daniel.Feliu@uclm.es, andres.sanmillanrodriguez@epfl.ch, Vicente.Feliu@uclm.es.

## Abstract

*This work is concerned with the mechanical design and the description of the different components of a novel mobile base for a flexible mobile manipulator. A flexible mobile manipulator is normally composed of multiple flexible links mounted on a mobile platform. This work is focused on the description of the mobile platform. The mobile platform of this work has two different configurations in order to carry out different tasks. Also, some hypothesis and experimental results are shown in this work as a first step to be able to obtain a kinematic model of the system later.*

**Keywords:** Kinematic model, orientation, posture, linear actuators, DC motors, identification.

## 1 INTRODUCTION

Compared to conventional robots, flexible link manipulators have the advantages of lower cost, larger work volume (they have longer links), higher operational speed, greater payload-to-manipulator-weight ratio, smaller actuators, lower energy consumption, better maneuverability, better transportability and safer operation due to reduced inertia. For these numerous advantages, extensive use of flexible manipulators in various robotic applications has made it as one of the research interests for many researchers over the world over the last few decades. Because energy consumption in motors is directly proportional to the mass and size of robot elements, long and light robot links are commonly used but which have a deformation that cannot be ignored. Some reviews of flexible robots can be found in [1] and [3].

There are many existing applications that take advantages of using lightweight links: in intervention robots, for hazardous waste cleanup, bomb disposal and refighting, maintenance of dangerous things (e.g hot electric power lines), mining robots, etc. Many of these applications use a mobile platform in order to transport the flexible manipulators.

Mobile manipulators have recently received con-

siderable attention and a wide range of applications have been explored. In most cases, a mobile robot needs some manipulation capability in order to be useful. For that reason, manipulators are mounted on mobile platforms.

These manipulators have usually power on board with limited energy due to the difficulty to store a great amount of energy in batteries. In this way, they reasonably make necessary the incorporation of light links in order to decrease the energy consumption. Another important advantage of using flexible manipulators is that due to their lightweight features, longer links can be designed in order to extend the workspace of the manipulators allowing them to reach targets that were, initially, outside of the manipulator workspace. An extensive literature survey on mobile manipulator system can be found in [2].

However the greatest disadvantage of these manipulators is the vibration problem due to low stiffness. This disadvantage makes very difficult the description of dynamics models and the design of control laws. Nevertheless, the importance and usefulness of these systems have engaged researchers worldwide in the investigation of these kind of systems. However, among different works that are carried out for mobile robotic arms, very few researches are dealt with the problem of modeling and control of mobile flexible manipulators (see [5] and [4]).

In this work, a new mechanical device able to transport a flexible robot, is presented. Its main features are: a) transport the flexible robot; b) increase the stability of the system when it reaches a specific target.

This article is organized as follows. Section 2 describes the mechanical design and the components of the system presented in this work. A control scheme for the linear actuators of the system is described in Section 3. Some experimental results are shown in Section 4. Finally some conclusions on the results are presented in Section 5.

## 2 MECHANICAL DESIGN

The system presented in this work is considered to be the mobile base of a flexible mobile manipulator. The platform consists of a rectangular base with four legs and four wheels (see Figure 1). The system described in this work is based in two different configurations in order to carry out two different tasks. The first configuration is when the system has the legs up and they are not in contact with the ground. In this configuration, the legs are not used and the system is used to transport the flexible manipulator from one place to another. The second configuration is when the system has the legs in contact with the field and in this case the wheels are not used. In this case, the system is used to control the orientation and the posture of the base of the flexible manipulator. Another function of this second configuration, is to increase the static stability of the system because when the mobile base reaches a particular target, the flexible manipulator which is on the mobile base is going to start moving.

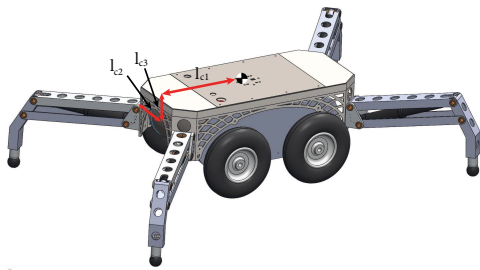


Figure 1: Front view of the experimental platform.

Therefore, the legs provide a solid base for the system. Their purpose is to improve the stability of the system during the operation of the flexible manipulator which is on the mobile base. They provide a solid platform for the flexible manipulator safe operation and efficient use. If the flexible manipulator has to be used, it is important to fully extend all of the legs and get the tires of the wheels off the ground.

The wheels do not offer the stability needed for the system, so the system needs the legs to prevent the system from leaning too much to one side or the other, or even overturn. This is the main purpose of adding four legs to our mobile platform. In the last decades, mobile cranes have used similar approaches in order to improve their stability. They use support devices called outriggers (see Figure 2). The outriggers normally use hydraulics to lift the entire crane, whereas our prototype uses linear actuator inside a mechanism that can be considered a four-link mechanism. The outriggers are

only one mechanism used to balance the crane during lifting operations. The legs prevent the system from tipping forward and backward during operation.



Figure 2: Mobile Crane. (image extracted from: <http://www.arnold.af.mil/News/Article-Display/Article/1192160/new-crane-purchased-to-support-national-defense-mission/>)

Each leg is actuated by a linear actuator which has the function to change the configuration of the system. Looking at Figure 3, we can see that modifying the extension of the linear actuator, the distance between the support point of the leg,  $P_D$ , and the point which joins the leg and the base of the truck,  $P_E$ , changes.

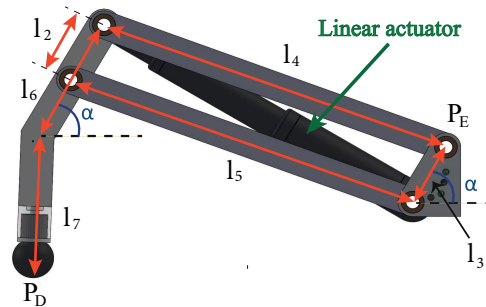


Figure 3: Scheme of a leg of the system.

In the Figure 3, it can be seen that each leg is a four-bar linkage which consists of four rigid bars in the plane connected by revolute joints. For analytical purposes, four bar linkages are treated as planar mechanisms. However, in practice, implementation of a four bar linkage could be spatial (non-planar). The four-bar linkage is the simplest and, often, the most useful mechanism. A variety of useful mechanisms can be formed from a four-link mechanism through slight variations, such as changing the character of the pairs, proportions of links, etc. As it was mentioned previously, the

objective of the four-bar linkage used in this work is to be able to modify the difference of height between  $P_D$  and  $P_E$  modifying the length of the linear actuator which is located in the middle of the four-bar system. Therefore, combining the movement of the four legs, we are able to modify the height and the posture (orientation) of the base of the system.

Figures 1 and 4 depict different views of the system and the rest of variables which define the features of the system. The values of these variables can be seen in Table 1.

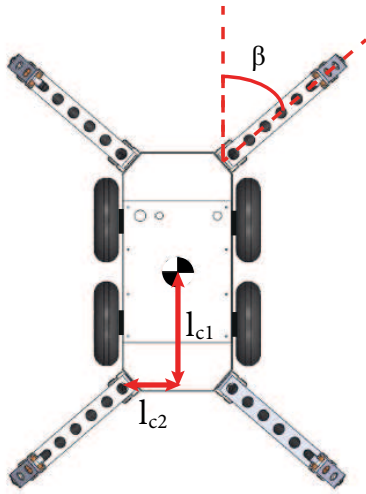


Figure 4: Top view of the experimental platform.

The parameters of the systems are:

Table 1: Parameters of the system

Parameters	Value
$l_{c1}$	400 mm
$l_{c2}$	170 mm
$l_{c3}$	113 mm
$l_2, l_3$	80 mm
$l_4, l_5$	440 mm
$l_6$	165 mm
$l_7$	205 mm
$\alpha$	$61^\circ$
$\beta$	$49^\circ$

## 2.1 COMPONENTS OF THE SYSTEM

This section describes the components of the system:

**One real-time high-performance embedded controller:** it is an advanced reconfigurable control and acquisition system. it includes a reconfig-

urable Field Programmable Gate Array (FPGA) chassis and it runs Labview Real-Time for control and analysis.

**One Module I/O Digitals (NI-9403 ):** This module is used to acquire the signal from the accelerometer, the encoders of the linear actuators and the twelve limit switches.

**One Module Voltage (NI-9264 ):** This module is used to send the control voltage signal to the two motor drivers in order to control the voltage in the linear actuators.

**Four linear actuators:** Linear actuators are electric devices able to convert rotational motion of a DC motor into linear pull/push movements. The actuators con50(14) are versatile, high efficiency, 12/24V DC industrial motors with planetary gears with small overall dimensions and a very high relation of reduction gear. They are made of powder-coated steel, providing a sturdy design that protects the motor and electric circuits. They are used to control the extension of the legs of the system (see Figure 3).

**Two motor drivers:** The Sabertooth 2x25 V2 are very versatile, efficient and easy to use dual motor drivers. The Sabertooth can supply two DC brushed motors with up to 25A each one. In our platform, each Sabertooth allows us to control two linear actuators with analog voltage, independently. Therefore, they will be used to control the position and the direction of the linear actuators.

**Four linear actuator encoders:** Each linear actuator has an encoder which measures the displacement of the linear actuators of the system. These sensors allow us to control the position and the speed of the linear actuators.

**Four Maxon DC motors set:** Each set is composed of Maxon DC motor which are high-quality motors fitted with powerful permanent magnets. Planetary reduction gears ( $n = 26$ ) and incremental high precision encoders with high signal resolution are mounted exclusively on motors with through shafts for resonance reasons. They are used to control the rotational movement of the wheels of the system.

**Four Positioning controllers (EPOS2 24/5):** They are small-sized smart motion controllers. Due to the flexible and high efficient power stage, the EPOS 24/5 drives brushed DC motors with digital encoder as well as brushless EC motors with digital Hall sensors and encoders. They integrate position, velocity and current controls which allow the user to develop sophisticated positioning applications. Each of these controllers is used to move one of the Maxon DC motors.

**Twelve limit switches:** These switches include electrical contacts with which to energize and de-energize a circuit. Four switches are located in order to detect the maximum extension of each leg and the other four switches are located in order to detect the maximum shrinkage of each leg. These eight switches are used in order to avoid the damage of the system when it surpasses its mechanical limits. Apart from that, the system has other four switches in order to detect when the leg is in contact with the field. This will be very important at the time the stabilization process is used.

**One inertial sensor:** The sensor is called ADIS16448 and it is a complete inertial system that includes a triaxial gyroscope, a triaxial accelerometer and a triaxial magnetometer. The sensor has been placed in the central part of the base of the truck in order to measure the orientation of the base of the platform.

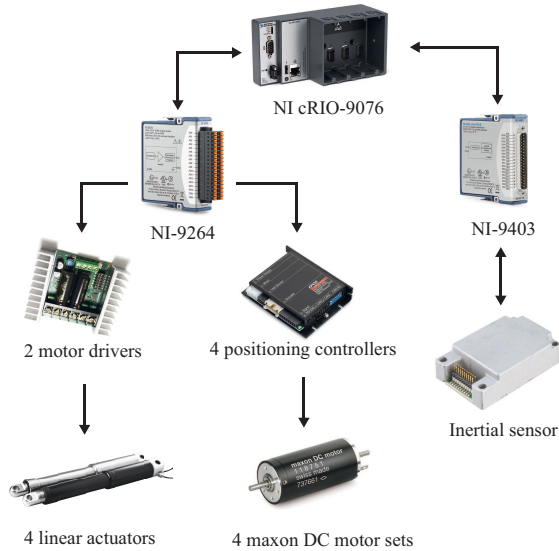


Figure 5: Components of the platform.

### 3 CONTROL OF THE LINEAR ACTUATORS

The definition of a mathematical model when the legs are in contact with the ground is of utmost importance in order to obtain advanced controllers that improve the control of the orientation and the posture of the base of the truck. The idea is to develop a simplified model based on a kinematic model of the system that relates the extension of the linear actuator with the orientation and posture of the system. This can be justified because the prototype when the legs are in contact with the ground moves at a slow speed. Therefore, the accelerations of the whole system are very small in

the stabilization phase which implies that inertial forces are very small in comparison with gravity forces. As a first step to develop the kinematic model of the system, we have to design controllers to control the extension of the linear actuators.

#### 3.1 LINEAR ACTUATOR DYNAMICS

The dynamic model of a typical DC motor is a very well known second-order equation. As it was explained previously, a linear actuator is a device that converts the rotational movement of a DC motor into linear movements. Therefore, the equation that describes the dynamics of a linear actuator can be expressed as:

$$\Gamma = K_m V = J_l \ddot{x} + \nu_l \dot{x} + \Gamma^{nlc} , \quad (1)$$

where  $\Gamma$  is the motor torque and it is assumed to be proportional to the control voltage signal  $V$ ,  $K_m$  is the constant that relates the motor torques with the control voltages,  $J_l$  and  $\nu_l$  are the equivalent inertia and the viscous friction of the system,  $\Gamma^{nlc}$  is the Coulomb friction of the motor and  $x$  is the linear position of the system. Therefore, the transfer function of the system considering the Coulomb Friction as a disturbance that will be canceled for the controller can be expressed as:

$$\frac{x}{V} = \frac{\frac{K_m}{J_l}}{s(s + \frac{\nu_l}{J_l})} , \quad (2)$$

#### 3.2 IDENTIFICATION OF THE SYSTEM

The identification process of the dynamics of the linear actuators was done for two different cases: a) when the leg is not in contact with the ground, therefore, the system does not have to move any load and b) when the system is in contact with the ground and it has the load of the mobile platform distributed among the four legs. In each case, ten steps with different amplitudes were used as input to the system. In Figures 6 and 7, the applied voltage of the system and the extension of the linear actuator are shown, respectively, for the case a). In Figures 8 and 9, the applied voltage of the system and the position of the linear actuator are shown, respectively, for the case b).

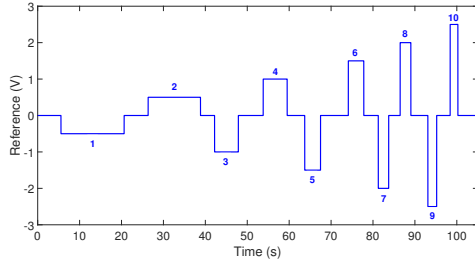


Figure 6: Applied voltage in case a).

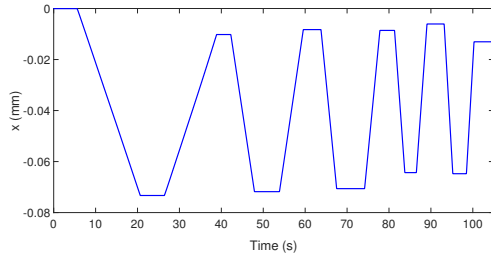


Figure 7: Extension of the linear actuator in case a)

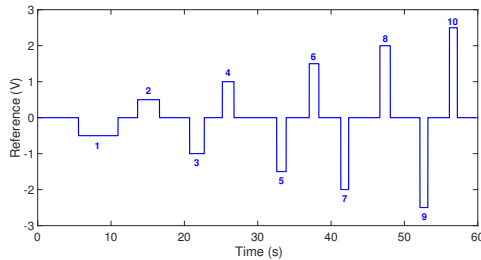


Figure 8: Applied voltage in case b).

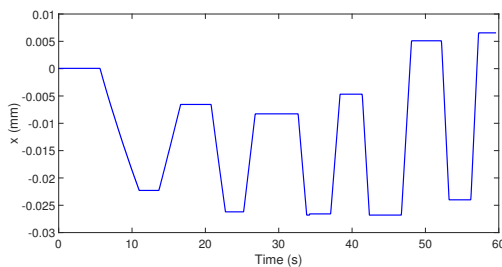


Figure 9: Extension of the linear actuator in case b)

From the previous figures, it can be concluded that the transfer function that relates the control signal ( $V$ ) and the linear position of the actuator ( $x$ ) for both cases, can be approximated by the expression:

$$G(s) = \frac{x(s)}{V(s)} = \frac{K}{s}; \quad (3)$$

It can be noticed that equation (2) tends to equation (3) if  $\frac{v}{J_t}$  is much higher than 1.

In Figure 10, the relation between the control signal and the velocity of the system can be shown for both cases.

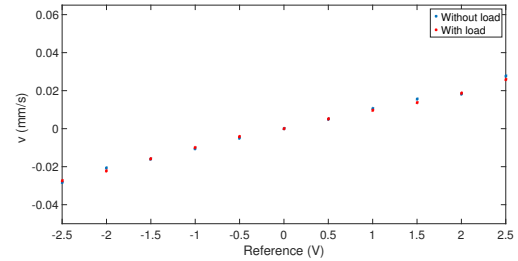


Figure 10: Relation between the control signal and the velocity.

The constant  $K$  of the transfer function (3) for each step and for both experiments can be seen in Figure 15:

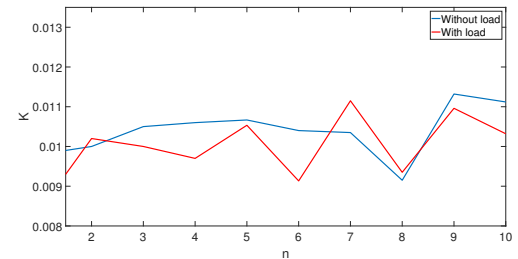


Figure 11: Estimation of the parameter  $K$  of the transfer function (3) .

The results show that the system has a similar behavior if the system has load or not. This phenomenon happens because the linear actuator has a very high reduction gear, therefore, the additional torque required to move a load has very slight influence in the dynamics of the system. Finally, it is obtained a nominal value of  $K = 0.01$  with a maximum variation of 15% for both experiments. This value was obtained doing the mean of  $K$  of the ten steps in both experiments. The same study was done for the other three legs obtaining similar results. Therefore, it was considered that the dynamics of the four legs of the system can be described using the transfer function (3) with a value of  $K = 0.01$ .

### 3.3 DESIGN OF THE CONTROLLERS

In our control system, we feed back measurements of the linear actuator positions  $x$ .

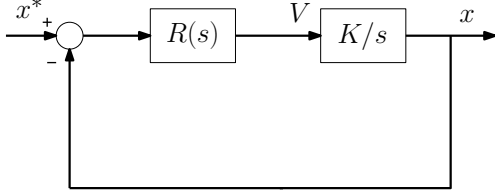


Figure 12: Control scheme.

We propose a controller with the form:

$$R(s) = \frac{K_p + K_v s}{s}; \quad (4)$$

Operating the characteristic polynomial (denominator of the closed-loop transfer function) of the system and equalizing to a second order transfer function:

$$H(s) = 1 + \frac{K_p + K_v s}{s} \frac{K}{s} = 0; \quad (5)$$

$$s^2 + K_p K_v s + K_p K_v = s^2 + 2ps + p^2; \quad (6)$$

where  $p$  is the absolute value of the position of the poles of the closed-loop transfer function. Therefore, from equation (6), we have two parameters and two equations.

## 4 EXPERIMENTAL RESULTS

This section shows some experimental results of using the proposed controllers of the linear actuators when the system is in contact with the ground in order to: a) demonstrate the efficiency of the proposed controllers for the linear actuators of the system and b) show how the orientation of the base of the truck changes when the four linear actuators move using a combined trajectory with the proposed control position. Figure 13 shows a photograph of the prototype.

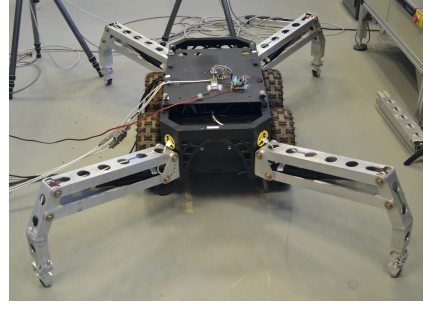


Figure 13: Experimental platform.

The method of describing the orientation of the frames used in this work will be the well-known roll ( $\phi$ ), pitch ( $\theta$ ) and yaw ( $\psi$ ) angles about fixed axes. This is the rotation about  $X$  by  $\phi$  (roll), rotation about  $Y$  by  $\theta$  (pitch) and about  $Z$  by  $\psi$  (yaw). The derivation of the equivalent rotation matrix  ${}^I_J R_{rpy}$  is straightforward because all rotations occur about axes of the reference frame:

$${}^I_J R_{rpy} = R_z(\psi)R_y(\theta)R_x(\phi) \quad (7)$$

$$R_z(\psi) = \begin{bmatrix} \cos \psi & -\sin \psi & 0 \\ \sin \psi & \cos \psi & 0 \\ 0 & 0 & 1 \end{bmatrix};$$

$$R_y(\theta) = \begin{bmatrix} \cos \theta & 0 & \sin \theta \\ 0 & 1 & 0 \\ -\sin \theta & 0 & \cos \theta \end{bmatrix};$$

$$R_x(\phi) = \begin{bmatrix} 1 & 0 & 0 \\ 0 & \cos \phi & -\sin \phi \\ 0 & \sin \phi & \cos \phi \end{bmatrix};$$

The different frames of the system can be defined (see Figure 14) as:

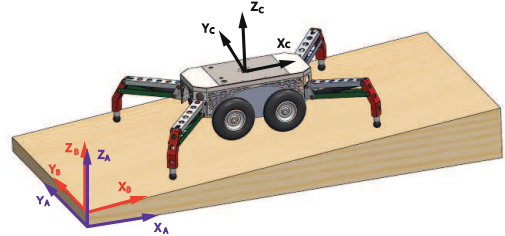


Figure 14: Experimental platform.

- Frame  $\{A\}$ : is the fixed frame of the system, its  $Z$  axis is parallel to the gravity force but

with opposite direction. This frame will be considered as the reference frame.

- Frame {B}: is a fixed frame of the surface where the system will be. Its Z axis is perpendicular to this surface. The orientation of this frame respect to {A} is  $[\phi_0 \theta_0 \psi_0]$ . It is assumed that during the stabilization process this frame is constant.
- Frame {C}: is an inertial frame, its Z axis is perpendicular to the upper part of the base of the truck. The orientation of this frame respect to {A} is  $[\phi(t) \theta(t) \psi(t)]$ . It is interesting to express the orientation of this frame respect to {A} because the inclination measurements of the sensor that will be used in the system are related to frame {A}. The origin of this coordinate frame is in the geometric center of the base of the truck.

Figures 15 and 16 show the results of using the control proposed in this work for the four parts. The poles of the controller were located in  $p = -10$  for the four linear actuators obtaining from equation (6) the following controller for the four linear actuators:

$$R(s) = \frac{2000s + 10000}{s}; \quad (8)$$

In Figure 15 the extension of the legs are shown, whereas in Figure 16 the two first components of the orientation of the base are shown. A camera-based optical tracking system was also used as an external sensor. This sensor consists of three infrared cameras which measures the orientation of the system with very high precision. Notice that, the third component is zero because the system does not rotate about the Z axis. In this Figure, we can see how the orientation of the system changes with the different extension of the legs.

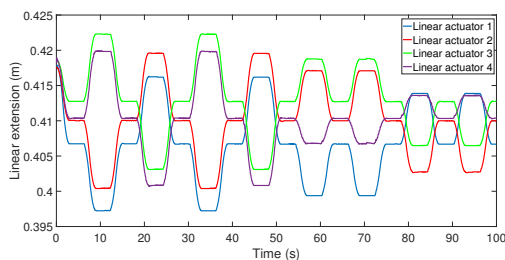


Figure 15: Extension of the linear actuators.

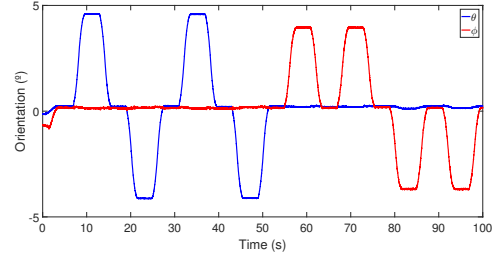


Figure 16: Orientation of the base of the platform

Finally, Figure 17 shows a nearly perfect tracking of the extension of a linear actuator is achieved.

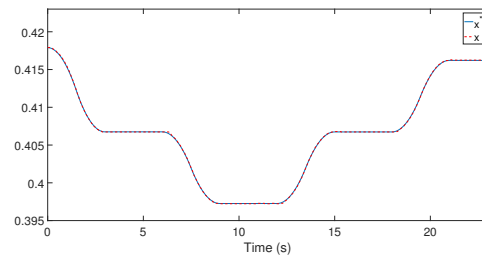


Figure 17: Response of the extension of a linear actuator.

## 5 CONCLUSIONS

We have presented a new mobile platform for flexible mobile manipulators. Its main features are that the system has legs and wheels in order to carry out two different tasks: a) transport a flexible manipulator from one place to another and b) increase the stability of the system being able to positionate the base of the platform with a specific posture and orientation. Also, it is proposed a control scheme for the extension of the linear actuators. Some experimental results show the efficiency of the proposed control scheme. It is important to highlight the importance of obtaining a precise model of the system in order to develop a control law for the posture and orientation of the system. The development of a kinematic model of the legs of the system in contact with the ground, that relates the extension of the actuators with the orientation of the base of the platform, will be the objective of our future research.

## Acknowledgement

This research was sponsored in part by the Spanish FPU14/02256 Program (Ministerio de Educación, Cultura y Deporte), in part by the Spanish State Research Agency and in part by the European Social Fund with the project DPI2016-

## References

- [1] BENOSMAN, M., AND LE VEY, G. Control of flexible manipulators: A survey. *Robotica* 22, 5 (2004), 533–545.
- [2] BLOCH, A., BAILLIEUL, J., CROUCH, P., MARSDEN, J. E., KRISHNAPRASAD, P. S., MURRAY, R., AND ZENKOV, D. *Non-holonomic mechanics and control*, vol. 24. Springer, 2003.
- [3] DWIVEDY, S. K., AND EBERHARD, P. Dynamic analysis of flexible manipulators, a literature review. *Mechanism and machine theory* 41, 7 (2006), 749–777.
- [4] KORAYEM, M. H., AND NOHOJJI, H. R. Trajectory optimization of flexible mobile manipulators using open-loop optimal control method. In *International Conference on Intelligent Robotics and Applications* (2008), Springer, pp. 54–63.
- [5] KUMAR, A., PATHAK, P. M., AND SUKAVANAM, N. Trajectory control of a two dof rigid–flexible space robot by a virtual space vehicle. *Robotics and Autonomous Systems* 61, 5 (2013), 473–482.



© 2018 by the authors.  
Submitted for possible  
open access publication  
under the terms and conditions of the Creative  
Commons Attribution CC-BY-NC 3.0 license  
(<http://creativecommons.org/licenses/by-nc/3.0/>).